第 24 卷第 5 期 无 机 化 学 学 报 Vol.24 No.5
2008 年 5 月 CHINESE JOURNAL OF INORGANIC CHEMISTRY 684~690

两个哒嗪衍生物为配体的铜(Ⅱ)配合物的合成、晶体结构和清除自由基活性

韩新利 李秀荣 于 丽 张智慧* 姜 萍
(南开大学化学学院化学系,天津 300071)

摘要:本文合成了 2 个新型 Cu(Ⅱ)配合物:$[Cu_2(L_1)_2Cl_4]L_1$ (**1**)和$[Cu(L_2)_2(NO_3)_2(H_2O)]$ (**2**),其中 L_1 为 3,6-二(苯并三唑-1-)哒嗪,L_2 为 3-(1,2,4-三氮唑-1-)-6-氯哒嗪。配合物 **1** 的晶体属于三斜晶系,$P\bar{1}$ 空间群。铜离子与 3 个氯原子和配体的 2 个氮原子形成五配位的四角锥构型,2 个氯原子以 μ-2 方式桥联 2 个中心铜原子。在配合物 **1** 的晶胞中 1 个游离配体未参与配位。配合物 **2** 的晶体属于单斜晶系,*C*2/*c* 空间群。铜原子处于五配位四角锥配位环境中。分子间氢键将 **2** 的分子结构延伸为一维链、二维网状结构,并通过分子间的 π-π 堆积作用进一步使配合物构型发展成三维拓扑结构。应用邻苯三酚自氧化法对本文所涉及的化合物进行了清除自由基活性测试,结果表明:这 2 个配体都具有较好的活性。

关键词:哒嗪;铜(Ⅱ)配合物;晶体结构;氢键;清除自由基活性
中图分类号:O614.121 **文献标识码**:A **文章编号**:1001-4861(2008)05-0684-07

Synthesis, Crystal Structures and Radical-scavenging Activities of Two Cu(Ⅱ) Complexes with the Ligand Containing Pyridazine Derivatives

HAN Xin-Li LI Xiu-Rong YU Li ZHANG Zhi-Hui* JIANG Ping
(*Department of Chemistry, Nankai University, Tianjin* 300071)

Abstract: Two Cu(Ⅱ) complexes, $[Cu_2(L_1)_2Cl_4]L_1$ (**1**) and $[Cu(L_2)_2(NO_3)_2(H_2O)]$ (**2**) (L_1 =3,6-bis-(benzotrizole-yl) pyridazine, L_2=3-(1,2,4-triazole-yl)-6-chloro-pyridazine), have been synthesized and characterized. The complex **1** crystallizes in the triclinic system, $P\bar{1}$ space group, the Cu(Ⅱ) ion is in five-coordinated square pyramidal coordinated environment with two N from the ligand and three Cl atoms. Two Cu(Ⅱ) ions are bridging linked by two Cl atoms in μ-2 model, and there is an uncoordinated ligand molecule in the unit cell of the complex **1**. The complex **2** crystallizes in the monoclinic system, *C*2/*c* space group, the Cu(Ⅱ) ion is also in a five-coordinated square pyramidal environment with two $N_{nitrate}$ atoms and three O_{water} atoms. The configuration of **2** is extended to 1D chain and 2D networks by hydrogen bonds, and then further extended to 3D topological framework via intermolecular π-π stacking action. The radical-scavenging activities of the title compounds have been studied by using the pyrogallol autoxidation method, the results indicate that the ligands present excellent radical-scavenging activities. CCDC: 641770, **1**; 649291, **2**.

Key words: pyridazine; copper(Ⅱ) complex; crystal structure; hydrogen bond; radical-scavenging activities

The chemistry of the poly-functional coordinated polymer and multi-nuclear complexes has become a fascinating area of research in the molecular construction and crystal engineering with the development of the novel functional material[1]. Moreover, the introduction of supramolecular interactions into specific polymeric

收稿日期:2007-09-02。收修改稿日期:2008-01-25。
*通讯联系人。E-mail:zhangzh67@nankai.edu.cn;Tel:(022)23501250
第一作者:韩新利,男,25 岁,硕士研究生;研究方向:功能配合物化学。

systems can lead to materials combining interesting architectures [2]. Among them, the design and synthesis of the function ligand is the most important factor for realizing the applications. Besides hydrogen-bonding which in the crystal engineering has resulted in a rapid expansion of interest in the topic[3,4], π-π stacking interactions are of certain interest[5]. Pyridazine and triazole and their derivatives are the important compounds in synthesis of farm drugs[6], medicine, and neuromuscular blocking activity[7] owing to the biological activities of these compounds.

We have reported two complexes of the pyridazine derivatives with a 3,5-dimethylpyrazole as a substitution group[8]. In the present work, two new pyridazine ligands contained substituted 1-H-1,2,4-triazole and benzotriazole group, respectively, and their copper(Ⅱ) complexes have been synthesized, and the radical-scavenging activities of the title compounds have been studied.

1 Experimental

1.1 Materials and general methods

All of the starting materials were of analytical grade and were used as received without further purification. Solvents were purified according to the standard methods prior to use. 1,2,4-triazole was synthesized by the literature method[9], FTIR. spectra were recorded on a Shimadzu IR-408 infrared spectrophotometer in the 4 000~400 cm^{-1} region. Elemental analyses of carbon, hydrogen and nitrogen were carried out with a Perkin-Elmer model 240 analyzer. Electronic spectra were recorded on a Shimadzu-u.v.-2450 spectrophotometer in the 200~800 nm range at room temperature.

1.2 Synthesis

1.2.1　3, 6-bis-(benzotrizole-yl)pyridazine (L_1)

The L_1 was prepared by modification literature method[10]. A solution of benzotriazole (2.28 g, 0.02 mol), PEG-400 (2.0 g), K_2CO_3 (5 g) and KI (1 g) were dissolved in 60 mL of acetone. In which, 3,6-dicholopyridazine (1.48 g, 0.01 mol) was added. The mixture was refluxing for 6 h, and then it was rotational evaporated. The crude products were re-crystallized from ethanol/water (V/V=1:1). A pale powder of L_1 was obtained. (Yield: 66.5% and m.p. 200 ℃). IR (KBr pellets, cm^{-1}): 3 143 (w), 3 083(s), 1 572(s), 1 549(m), 1 461 (s), 1 427(s), 1 390(s), 1 320(w), 1 289(s), 1 241(w), 1 180 (s), 1 054(s), 953(w), 844(s), 779(s), 653(w), 575(w). Elemental analyses: Found (%): C, 61.05; H, 3.32; N, 35.59. $C_{16}H_{10}N_8$, calcd(%).: C, 61.14; H, 3.21; N, 35.65.

1.2.2　3-(1,2,4-triazole-yl)-6-chloro-pyridazine (L_2)

The L_2 was prepared by modification literature method[11]. 1-H-1,2,4-triazole4 (4.2 g, 0.061 mol) and NaOH (2.44 g, 0.061 mol) were dissolved in ethanol (50 mL), and then 3,6-dicholopyridazine(9.10 g, 0.061 mol) were added with stirring, the reaction was kept running for 4h.under reflux. The reaction solution was filtered, rotation evaporated. The powders of L_2 were obtained by re-crystallizing from chloroform. (Yield: 50.2% and m. p. 180~182 ℃). IR. (KBr pellets, cm^{-1}): 3 104(m), 3 070 (m), 1 572(m), 1 513(s), 1 445(s), 1 372(m), 1 286(m), 1 145(s), 1 032(m), 977(w), 860(m), 777(w), 674(m), 529 (w). Elemental analyses: Found (%): C, 39.55; H, 2.35; N: 38.42. $C_6H_4ClN_5$ calcd (%): C, 39.69; H, 2.22; N, 38.57.

1.2.3　$[Cu_2(L_1)_2Cl_4]L_1$ (**1**)

A buffer solution (6 mL) of chloroform and methanol (V/V=1:1) was carefully layered over the solution of L_1 (0.05 mmol) in chloroform. Then a solution of $CuCl_2$ (0.1 mmol) in methanol was layered over the buffer layer. Purple-red crystals of **1** suitable for X-ray analysis were obtained after *ca.* one month. Yield: 43.2%. IR (KBr pellets, cm^{-1}): 3 091(w), 3 046(w), 1 607 (m), 1 555 (m), 1 470 (s), 1 438 (s), 1 295 (s), 1 241(w), 1 205(w), 1 076(m), 1 063(m), 1 024(s), 852(m), 785(s), 742 (s), 578 (w). Elemental analyses: Found (%): C, 50.29; H, 2.75; N, 29.30. $C_{32}H_{20}Cl_2CuN_{16}$ calcd. (%): C, 50.37; H, 2.64; N, 29.37.

1.2.4　$[Cu(L_2)_2(NO_3)_2(H_2O)]$ (**2**)

For **2**, the same procedure was run as that of **1**, except L_2 was used instead of L_1, and $Cu(NO_3)_2$ was used instead of $CuCl_2$, respectively. Blue single crystals of **2** suitable for X-ray analysis were obtained after *ca.* six weeks. Yield: 48.6%. IR (KBr pellets, cm^{-1}): 3 143(m), 3 076(br), 1 571(m), 1 525(m), 1 479(m), 1 454(s), 1 407 (s), 1 382(vs), 1 290(m), 1 143(s), 1 041(m), 971(m), 837

(m), 779 (w), 665 (m) cm^{-1}. Elemental analyses: Found (%): C, 25.28; H, 1.85; N, 29.49. $C_{12}H_{10}Cl_2CuN_{12}O_7$ calcd (%): C, 25.34; H, 1.77; N, 29.55.

1.3 Crystal structure determination of complexes (1) and (2)

The crystals with dimensions of 0.20 mm × 0.18 mm × 0.14 mm for complex **1** and 0.28 mm × 0.18 mm × 0.14 mm for complex **2** were carefully selected for structure determination. All the data were collected on a Bruker Smart CCD diffractometer with graphite monochromatized Mo $K\alpha$ radiation (λ=0.071 073 nm)at room temperature using the ω-2θ scan technique. The structure was solved by the direct method and subsequent difference Fourier syntheses and refined on F^2 by a full-matrix least-squares method. The non-hydrogen atoms were refined anisotropically and hydrogen atoms were included in the structure factor calculation but not refined. All the calculations were carried out with SHELXS-97 and SHELXL-97 programs[12]. The crystal data and data collection details are summarized in Table 1.

CCDC: 641770, **1**; 649291, **2**.

Table 1 Crystal data and structure refinement for complexes 1 and 2

Compound	**1**	**2**
Empirical formula	$C_{32}H_{20}Cl_2CuN_{16}$	$C_{12}H_{10}Cl_2CuN_{12}O_7$
Formula weight	763.08	568.76
Temperature / K	294(2)	294(2)
System	Triclinic	Monoclinic
Space group	$P\bar{1}$	*C*2/*c*
a / nm	0.815 3(3)	2.848 9(4)
b / nm	0.878 0(3)	0.682 67(10)
c / nm	2.329 1(7)	1.1373 4(16)
α / (°)	95.967(5)	
β / (°)	93.330(6)	113.224(2)
γ / (°)	105.005(5)	
V / nm^3	1.595 3(8)	2.032 7(5)
Z	2	4
Crystal size / mm	0.20×0.18×0.14	0.28×0.18×0.14
D_c / ($g\cdot cm^{-3}$)	1.589	1.858
μ(Mo $K\alpha$) / mm^{-1}	0.906	1.406
F(000)	774	1 140
2θ range / (°)	0.88~26.62	3.08~26.40
Reflections collected	8 301	5 612
Indep. refls. (Rint)	5 621 (0.029 8)	2 080 (0.024 4)
Observed reflections	3 706	1 789
GOF on F^2	1.045	1.08
Data / restraints / parameters	5 621 / 0 / 460	2 080 / 1 / 159
Final R_1 and wR_2 [$I>2\sigma(I)$]	0.046 0, 0.106 5	0.028 9, 0.074 8
R_1 and wR_2 [all data]	0.086 7, 0.134 0	0.036 4, 0.078 9
Largest diff. peak and hole / ($e\cdot nm^{-3}$)	370 and −534	386 and −353

1.4 Radical-scavenging activities measurement

The radical-scavenging activities of the ligands and complexes have been tested using the pyrogallol autoxidation method[13]. For the controlling test: The Tris-HCl buffer (5 mL, pH=8.2) was mixed with double distillated water (5 mL), and the mixture were kept at 25±0.2 ℃ for 20 min. Then 0.3 mL of pyrogallol solution (3 $mmol\cdot dm^{-3}$) in HCl (0.1 $mmol\cdot dm^{-3}$) was added to the mixture with stirring, the solution was quickly transferred to the cell for the absorption measurement at

325 nm on a SHIMADZU UV-2450 spectrophotometer. The plots of absorptions vs time (s) were obtained and the slope of the line is the autoxidizing velocity of pyrogallol.

For the ligands and complexes: the solution of the samples with different concentrations was kept at 25±0.2 ℃ for 20 min, respectively. To every solution, 0.3 mL of pyrogallol solution (3 mmol·dm^{-3}) was added and run using the same procedures as for pyrogallol samples. The plots on the absorption data of pyrogallol by the action of the compounds with various concentrations vs time (s) were made. The autoxidizing velocity of pyrogallol after adding the compounds with various concentrations can be obtained from the slopes of the lines.

2 Result and discussion

2.1 Synthesis of the title compounds

For the ligand L_1, a mixture of the symmetrical and asymmetrical configurations has been obtained by the methods mentioned above without further separation (Chart 1), which leads to two coordinated models of the benzotriazole group in the complex **1**.

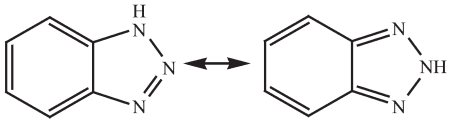

Chart 1　Molecular structure of the benzotriazole isomer

In the process of preparation of the metal complexes, the precipitates of the metal complexes are easy to generate due to the strong coordination ability of the triazole groups on the ligands. Thus, the layered diffusion method is used to synthesize the metal complexes rather than the solvent evaporation method at room temperature.

2.1.1　Crystal structure of $[Cu_2(L_1)_2Cl_4]L_1$ (**1**)

An OPTEP view of **1** is shown in Fig.1. Selected bond distances and angles are given in Table 2. In the compound **1**, the copper atom is in a five-coordinated square pyramidal environment. Take Cu(1) as an example, Cl(1) atom is located on the apical position with an elongated Cu-Cl distance Cu(1)-Cl(1) 0.268 02(13) nm, and Cl(1A), N(1), N(4), and Cl(2) atoms define the basal plane, among them, Cl(2) is a little depart from the plane Cl(2)-Plane$_{Cl(1A),N(1),N(4)}$ 0.055 8 nm. The bond distance of Cu-Cl (1) 0.268 02 nm is slight longer than that of Cu-Cl(1A) and Cu-Cl(2) [Cu-Cl(1A) 0.225 09 nm, Cu-Cl(2) 0.222 7 nm]; the distance of Cu(1)-$N_{triazole}$ [0.206 1(3) nm] is slightly longer than that of Cu(1)-$N_{pyridazine}$ [0.204 6(3) nm], all of them are normal bonds. Two Cu atoms and two Cl atoms construct a rectangle, and two [Cu(L_1)Cl] units are bridging linked by two Cl atoms in μ-2 model. It is noticed that there is an uncoordinated L_1 molecule in the unit cell of the complex **1**. The Cl atoms present two kinds of coordination modes, one is a terminal mono-dentate coordinated mode, the other is μ-ClXCl bridge mode. A four-member ring [Cu_2Cl_2] with Cu⋯Cu separation 0.338 4 nm, namely a second building unit (SUB)[14], which is the basic unit to extend the structure to 2D networks by H-bonds (Table

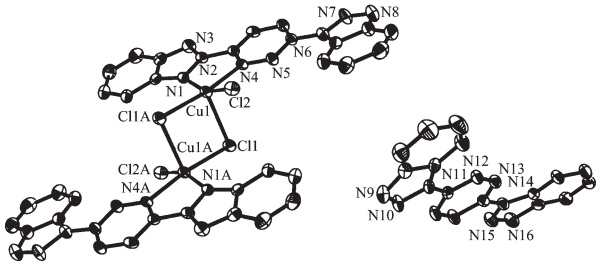

Symmetry operate: 1−*x*, −*y*, −*z*

Fig.1　Perspective view of the coordination environment of Cu(Ⅱ) in **1**, H atoms are not shown for clarity

Table 2　Selected bonds lengths (nm) and angles (°) for 1

Cu(1)-N(1)	0.206 1(3)	Cu(1)-Cl(1)#1	0.225 09(11)	Cu(1)-N(4)	0.204 6(3)
Cu(1)-Cl(1)	0.268 02(13)	Cu(1)-Cl(2)	0.222 70(12)	Cl(1)-Cu(1)#1	0.225 08(11)
N(4)-Cu(1)-N(1)	78.36(12)	N(4)-Cu(1)-Cl(1)	89.65(9)	N(4)-Cu(1)-Cl(2)	92.49(10)
N(1)-Cu(1)-Cl(1)	90.82(9)	N(1)-Cu(1)-Cl(2)	160.03(9)	Cl(2)-Cu(1)-Cl(1)	107.00(4)
N(4)-Cu(1)-Cl(1)#1	170.64(9)	Cl(1)#1-Cu(1)-Cl(1)	93.80(4)	N(1)-Cu(1)-Cl(1)#1	92.88(9)
Cu(1)#1-Cl(1)-Cu(1)	86.20(4)	Cl(2)-Cu(1)-Cl(1)#1	94.82(5)		

Symmetry transformations used to generate equivalent atoms: #1: −*x*+1, −*y*, −*z*.

Table 3 H-bonding geometry for 1[a]

D–H···A	D-H / nm	H···A / nm	D···A / nm	D–H···A / (°)
C(13)–H(13)···N(10)^{i}	0.093 0	0.273 7	0.344 0	115.93
C(8)–H(8)···Cl(2)^{ii}	0.093 0	0.268 8	0.340 2	134.12

[a] Symmetry code: ^{i} $x-1, y, z$; ^{ii} $x, y-1, z$.

3). The Cu···Cu separations are 0.878 0 nm and 0.485 2 nm, respectively (Fig.2).

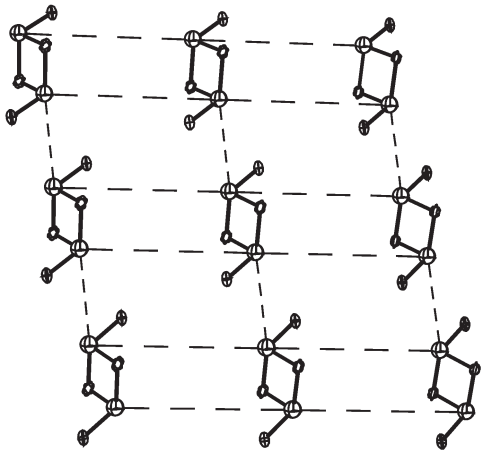

All C, N atoms omitted for clarity

Fig.2 2D networks of complex **1**

2.1.2 Crystal structure of $[Cu(L_2)_2(NO_3)_2(H_2O)]$ (**2**)

The molecular structure of **2** is shown in Fig.3, and the selected bond distances and the angles are summarized in Table 4. It can be seen from Fig.3 that the copper (Ⅱ) is in a five-coordinated square pyramidal environment with two nitrogen atoms from L_2 and two $O_{nitrate}$ and one O_{water}. The O (4) is located on the apical position with a normal Cu-O distance 0.228 3 (3) nm, and O(1), O(1A),N(1),N(1A) atoms defining the basal plane are just constructed a rectangle with the angle of N(1A)- O(1)-N(1) being 90.15° and the angle of O(1)-N(1)-O(1A) being 89.82°. The adjacent $[Cu(L_2)_2(NO_3)_2(H_2O)]$ molecules are arranged to present an 1D chain through H-bond, the bond distance of O (4B)-O (2A) is 0.296 8 nm and the angle of O(4B)–H(4A)···O(2A) is 127.24°. The 1D chain crosses each other to develop the repeat units to 2D networks (Fig.4) by hydrogen bond which data are summarized in Table 5.

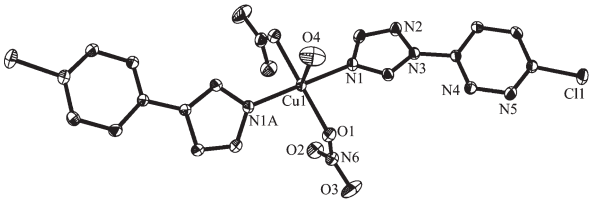

Symmetry operate: $-x, y, 3/2-z$

Fig.3 ORTEP view of the complex **2**, omitting H atoms for clarity

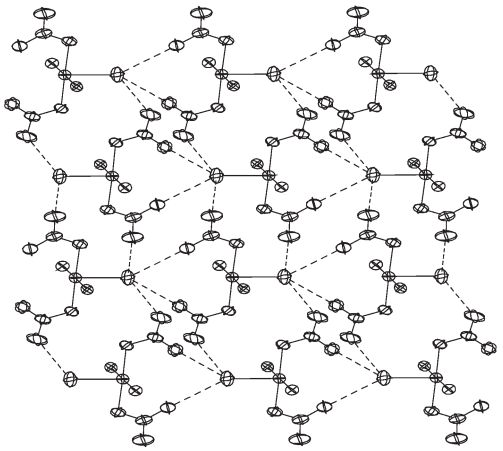

C atoms and part of N atoms omitted for clarity

Fig.4 Networks formed by H-bongs in **2**

From the Fig.4, it can be seen that every two Cu(Ⅱ) centers are linked to form a ten-member macrocycle by

Table 4 Selected bonds lengths (nm) and angles (°) for 2

Cu(1)-O(1)#1	0.198 93(15)	Cu(1)-N(1)	0.199 52(16)	Cu(1)-O(1)	0.198 93(15)
Cu(1)-O(4)	0.228 3(3)	Cu(1)-N(1)#1	0.199 52(16)		
O(1)#1-Cu(1)-O(1)	178.84(9)	N(1)#1-Cu(1)-N(1)	178.67(10)	O(1)#1-Cu(1)-N(1)#1	88.99(7)
O(1)#1-Cu(1)-O(4)	89.42(5)	O(1)-Cu(1)-N(1)#1	91.02(7)	O(1)-Cu(1)-O(4)	89.42(5)
O(1)#1-Cu(1)-N(1)	91.02(7)	N(1)#1-Cu(1)-O(4)	90.67(5)	O(1)-Cu(1)-N(1)	88.99(7)
N(1)-Cu(1)-O(4)	90.67(5)				

Symmetry transformations used to generate equivalent atoms: #1: $-x, y, -z+3/2$.

Table 5　H-bonding geometry for 2[b]

D–H···A	D-H / nm	H···A / nm	D···A / nm	D–H···A / (°)
O(4B)–H(4A)···O(2A)^{i}	0.083 9	0.238 4	0.296 8	127.24
O(4B)–H(4AA)···O(2AA)^{ii}	0.083 9	0.238 4	0.296 8	127.24
O(4B)–H(4A)···O(3A)^{iii}	0.083 9	0.238 4	0.321 2	142.4
O(4B)–H(4A)···O(3AL)^{iv}	0.083 9	0.238 4	0.321 2	142.4
C(5A)–H(5A)···N(5T)^{v}	0.093 0	0.287 1	0.337 0	114.91
C(4A)–H(4A)···N(4AK)^{vi}	0.093 0	0.251 0	0.338 0	155.74
C(4A)–H(4A)···N(5AK)^{vii}	0.093 0	0.252 4	0.320 5	130.31

[b]Symmetry code: ^{i} x, $y-1$, z; ^{ii} $-x$, $y-1$, $z-1$; ^{iii} $-x$, $-y$, $-z-1$; $^{iv, v, vi, vii}$: x, y, z.

hydrogen bond, and two copper(Ⅱ) centers are linked through the water and the nitrate group to present a eight-member ring structure. The 2D networks are developed to a 3D architecture through the intermolecular π-π stacking weak interactions (Fig.5) between pyradizine-pyradizine rings with the centroid-centroid separation of 0.371 1 nm and dihedral angle of 0°, which further stabilize the structure of **2**.

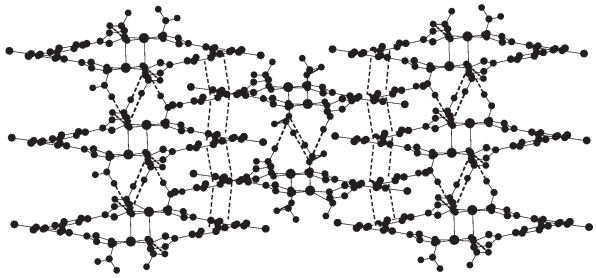

Fig.5　3D architecture linked by intermolecular π-π stacking interactions

In the comparison of the molecular structure of **1** with that of **2**, it can be seen that two coordinated N atoms come from benzotrizole and pyridazine in **1**, while in **2**, only one N atom of triazole coordinates to the metal centers. The corresponding bond lengths of metal-$N_{trizole}$ in **1** are longer than those in **2**, it might be due to the stereo inhibition of benzotrizole molecule. It is noticeable that there is an uncoordinated ligand, in which two benzotrazoles are linked to pyridazine in symmetric mode, while the coordinated L_1 is asymmetric mode. The result indicates that the coordinated ability of the asymmetric benzotriazole is stronger than that of the symmetric one in L_1.

2.2　Radical-scavenging activities of the title compounds

The autoxidizing velocity of pyrogallol, r_0, and the autoxidation of pyrogallol after adding L with various concentrations are shown in Fig.6(a), 6(b), and 6(c), respectively. The autoxidizing velocities of pyrogallol with various concentrations of L, r_i, are summarized in Table 6. It is found that the greater the concentration of L, the lower the velocity of pyrogallol autoxidizing. The IC_{50} value of L_1 and L_2 is 29.53 μg·mL^{-1} and 32.76 μg·mL^{-1}, respectively, which indicates that the L_1 and L_2 have potential radical-scavenging activities. The inhibition rate (η) is calculated by the formula: $\eta=1-r_i/r_0$. The radical-scavenging activities of the metal complexes **1** and **2** are not obvious, which might be due to the

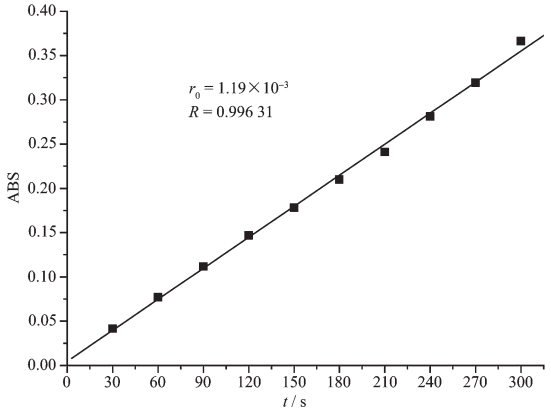

Fig.6(a)　Velocity of self-oxidazing of pyrogallol

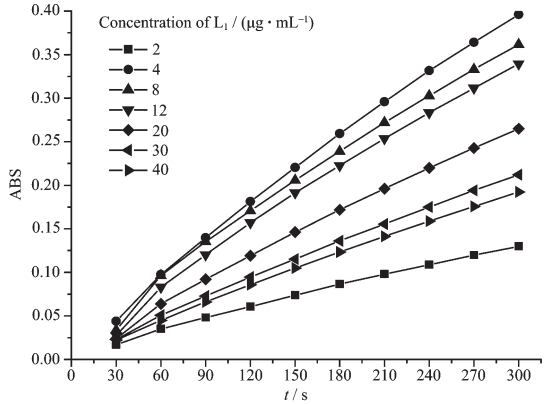

Fig.6(b)　Plots on the absorption (A) of pyrogallol by the action of L_1 with concentrations vs time

Table 6 Inhibition of L_1 and L_2 to the autoxidation of pyrogallol

L_1 concentration / ($\mu g \cdot mL^{-1}$)	r_i / 10^{-4}	η / %	L_2 concentration / ($\mu g \cdot mL^{-1}$)	r_i / 10^{-4}	η / %
2	11.5	2.540	2	11.7	0.847
4	10.4	11.86	4	11.2	5.084
8	8.82	25.25	8	9.59	18.73
12	7.09	39.91	12	8.72	26.10
20	6.44	45.42	20	6.91	41.44
30	5.81	50.76	30	6.25	47.03
40	5.08	56.94	40	4.12	65.08

generation of some color species to interrupt the rule of the pyrogallol autoxidation[15].

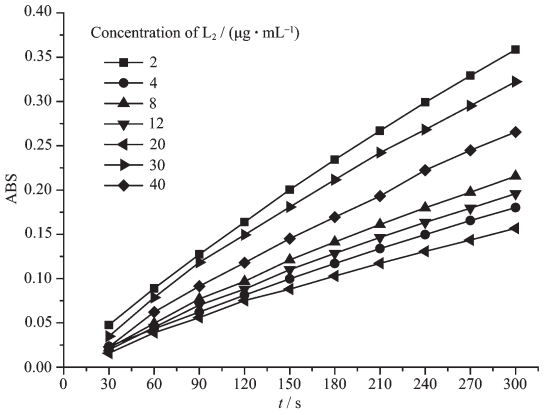

Fig.6(c) Plots on the absorption (A) of pyrogallol by the action of L_2 with concentrations vs time

3 Conclusion

In this work, we have reported two copper (Ⅱ) complexes with the pyridazine derivatives ligands, $[Cu_2(L_1)_2Cl_4]L_1$ (**1**) and $[Cu(L_2)_2(NO_3)_2(H_2O)]$ (**2**). The molecular structures of the copper (Ⅱ) complexes are different due to stereo influences of the substituted groups on the pyridazine ring, and hydrogen bond and π-π sticking action are important for the construction of the coordinated polymers. The radical-scavenging activities of the ligands and complexes have been studied, and the results indicate that two ligands present excellent radical-scavenging activities.

References:

[1] (a)Mandal S K, Thomopson L K, Gabe E J, et al. *Inorg. Chem.*, **1987**,**27**: 855~859

(b)Ardizzoia G A, Cenini S, Monica G L, et al. *Inorg. Chem.*, **1994**,**33**:1458~1463

[2] Brunsveld L, Folmer B, Meijer E W, et al. *Chem. Rev.*, **2001**, **101**:4071~4097

[3] Zaworotko M J. *Chem. Soc. Rev.*, **1994**,**23**:283~288

[4] Batsanov A S, Hubberstey P, Russell C E, et al. *J. Chem. Soc., Dalton Trans.*, **1997**:2667~2672

[5] GUO Hui-Rui(郭辉瑞), TAO Zhu(陶 朱), ZHU Qian-Jiang(祝黔江), et al. *Chinese J. Inorg. Chem.*(*Wuji Huaxue Xuebao*), **2002**,**18**(5):436~441

[6] Tavares F X, Boucheron J A, Dickerson S H, et al. *J. Med. Chem.*, **2004**,**47**(19):4716~4730

[7] Steck B E A, Bruline R, Fletcher L T. *J. Am. Chem. Soc.*, **1954**,**76**:4454~4457

[8] GAO Hong, ZHANG Zhi-Hui, JIANG Ping, et al. *Transition Metal Chem.*, **2006**,**31**:1088~1092

[9] DU Bin(杜 斌). *Chinese J. of Pharmaceuticals.*(*Zhongguo Yiyao Gongye Zazhi*), **2000**,**31**(11):515~515

[10]XIE Xiao-Juan(谢筱娟), CHENG Lin(程 林), ZHENG Ai-Hua(郑爱华), et al. *Synthesis Chemistry*(*Hecheng Huaxue*), **2000**,**8**(3):252~255

[11]TANG Chu-Chi(唐滁痴), LI Yu-Chang(李虞昌), CHEN Bin(陈 彬). *Pesticide Chemistry*(杀虫剂化学). Tianjin: Nankai University Press, **1998**.

[12](a)Sheldrick G M. *SHELXS*-97, *Program for Crystal Structure Solution*, University of Göttingen, **1997**.

(b)Sheldrick G M. *SHELXL*-97, *Program for Crystal Structure Refinement*, University of Göttingen, **1997**.

[13]Castellano R K, Diederich F, Meyer E A. *Angew. Chem. Int. Edn.*, **2003**,**42**(11):1210~1250

[14]MA Ai-Qing, ZHU Long-Guan. *Transition Metal. Chem.*, **2005**,**30**:869~872

[15]Marklund S, Marklund G. *Eur. J. Biochem.*, **1974**,**47**:469~474